THE ANATOLIAN JOURNAL OF CARDIOLOGY

Official journal of the TURKISH SOCIETY OF CARDIOLOGY

Bioinformatic Analysis and Molecular Docking Identify Isorhamnetin Is a Candidate Compound in the Treatment of Pulmonary Artery Hypertension

ABSTRACT

Background: The current study aims to identify the key pathways and potential therapeutic targets for pulmonary arterial hypertension (PAH) and to further evaluate the anti-PAH effects of isorhamnetin.

Methods: The dataset of gene expression profiling for PAH (GSE113439) was downloaded from the gene expression omnibus (GEO) database. Isorhamnetin target genes were extracted from the comparative toxicogenomics database (CTD). Various bioinformatics methods were employed to identify the core pathways associated with PAH and potential intervention targets. Molecular docking was conducted between the interacting target and the candidate compound, isorhamnetin.

Results: One thousand nine hundred sixty-two upregulated genes and 642 downregulated genes were identified. Molecular complex detection analyses revealed that the signifi ant biological processes associated with upregulated genes included DNA damage response, mitotic cell cycle, and chromosome organization. In contrast, the signifi ant biological processes related to downregulated genes encompassed cellular response to growth factor stimulus, response to growth factor, and blood vessel development. Immune infilt ation analysis indicated that PAH is associated with signifi ant changes in the distribution of immune cells and differential expression of immune checkpoints. Furthermore, 58 isorhamnetin targets were extracted from the CTD, and we identified 1 interacting gene, *NFE2L2*, among the differentially expressed genes (DEGs), DEGs related to ferroptosis, and isorhamnetin targets. Isorhamnetin demonstrated strong affinities with vascular endothelial growth factor (VEGF) receptors and transcription factors (*ATM* and *ZNF24*) associated with VEGFs, as well as the ferroptosis protein NFE2L2.

Conclusions: Pulmonary arterial hypertension is characterized by a series of abnormalities in downstream molecular signaling pathways, including DNA damage, immune dysregulation, VEGF signaling deficienc , and the ferroptosis process. These may represent the core pathophysiological mechanisms of PAH. Ferroptosis-related genes, such as *NFE2L2* and TF (*ATM, ZNF24*) associated with VEGFs, are potential therapeutic targets that contribute to the mechanisms mentioned above. Isorhamnetin is a promising candidate compound for the treatment of PAH.

Keywords: Pulmonary artery hypertension, bioinformatics, molecular docking, immune infilt ation, isorhamnetin

INTRODUCTION

Pulmonary artery hypertension (PAH) is a severe, progressive disease that results in ongoing right ventricular remodeling and right heart failure. Pulmonary artery hypertension is characterized by increased pulmonary vascular resistance (PVR), arterial remodeling, *in situ* pulmonary arterial thrombosis (ISPAT), and stiffness of the pulmonary vascular walls. These pathological features are associated with multiple mechanisms, including endothelial damage, dysregulation of the immune system, and ionic metabolic abnormalities.[1] The survival rate of PAH patients, confirmed for the fir t time, is approximately 60% over a 3-year period. Pulmonary artery hypertension is often referred to as the "cancer" of the cardiovascular system.[2] Consequently, exploring the fundamental pathological pathways, identifying

ORIGINAL INVESTIGATION

Chen Shao[1]
Wei Xia[2]
Yang Liu[3]

[1]*Department of Nursing Science, The Second People's Hospital of Lianyungang, Jiangsu, China*
[2]*Department of Pharmacology, The Second People's Hospital of Lianyungang, Jiangsu, China*
[3]*Department of Internal and Pediatrics, School of Clinical Medicine, Qilu Medical University, Zibo, Shandong, China*

Corresponding author:
Yang Liu
✉ 13009726899@163.com

Received: August 3, 2024
Accepted: October 18, 2024
Available Online Date: November 27, 2024

Cite this article as: Shao C, Xia W, Liu Y. Bioinformatic analysis and molecular docking identify isorhamnetin is a candidate compound in the treatment of pulmonary artery hypertension. *Anatol J Cardiol.* 2024;XX(X):1-14.

DOI:10.14744/AnatolJCardiol.2024.4723

therapeutic targets, and screening potential chemical candidates for PAH are crucial for early diagnosis and treatment.

The mechanisms of PAH have been extensively studied in recent years; however, therapeutic targets and preventive methods have not yet been fully identified. Ferroptosis is a newly discovered form of cell death that differs from necrosis, apoptosis, and autophagy.[3] It is primarily induced by iron-dependent lipid peroxidation, which leads to mitochondrial contraction, rupture of the mitochondrial membrane, cellular respiratory dysfunction, energy metabolism deficienc , and DNA damage.[4,5] Previous studies have demonstrated that pulmonary vascular remodeling is influen ed by factors such as oxidative stress, lipid peroxidation, and infla - mation, all of which share molecular characteristics with the ferroptosis process.[4,5] Additionally, it has been found that the activation of ferroptosis signaling coincides with the onset of idiopathic PAH.[4] Ferroptosis is not only associated with heart and lung diseases, such as myocardial infarction and chronic obstructive pulmonary disease, but also plays a role in the pathogenesis and progression of PAH.[6-8] However, the precise role of ferroptosis in the pathological mechanisms of PAH remains unclear.

In recent years, approximately 4000 plant-derived fla onoid compounds have been identified, many of which possess a variety of medicinal properties.[9] Isorhamnoin is a specific class of fla onoid compounds primarily extracted from the fruits of "*Hippophae rhamnoides*" and the leaves of "*Ginkgo biloba L.*" Isorhamnoin exhibits anti-inflamma ory and antioxidant effects and has the ability to protect vascular endothelial cells. Accumulating evidence suggests that isorhamnoin, as a supplemental agent, can be utilized to treat various diseases due to its pharmacological activities, including cardiovascular and cerebrovascular protection, anti-tumor effects, anti-inflamma ory properties, antioxidant activity, organ protection, and obesity prevention.[10-15] These studies indicate that isorhamnoin may be a promising candidate for combating PAH. Therefore, we conducted an integrated bioinformatics analysis and network pharmacology approach to investigate the core therapeutic targets of PAH, extending to ferroptosis signaling, and further assessed the anti-PAH effects.

METHODS

Dataset

We conducted a gene expression profiling analysis of pulmonary arterial hypertension (GSE113439) using the gene expression omnibus (GEO) database (www.ncbi.nlm.nih.gov/geo/). This study employed microarray analysis to examine the gene expression profiles of patients with PAH compared to normal controls. The samples were collected from the tissues of 15 PAH cases, which included 6 cases of idiopathic PAH, 4 cases of PAH secondary to connective tissue disease, 4 cases of PAH secondary to congenital heart disease, and 1 case of chronic thromboembolic pulmonary hypertension. Additionally, 11 normal control samples were obtained from lung tissue adjacent to lung cancer resections.[16]

Differentially Expressed Genes

All microarray data were downloaded from the GEO database (http://www.ncbi.nih.gov/geo). The data are standardized, and the raw files were obtained in MINiML format. The limma package in the R software was employed to analyze the differentially expressed mRNAs (R software is developed by Synopsys in the United States). The adjusted *P*-value was assessed to correct for false positive results in the GEO datasets. A threshold of "Adjusted $P < .05$ and |Log2 Fold Change| > 1.5" was established to define the differential expression of mRNAs.[17]

Ferroptosis

Microarray data were downloaded from the GEO database (http://www.ncbi.nih.gov/geo). The raw data were obtained in MINiML format. Ferroptosis-related genes were identified from Liu et al's[18] systematic analysis of the aberrances and functional implications of ferroptosis in cancer. The analysis was conducted using statistical package for social sciences (SPSS) software (version 20.0). We used the Kolmogorov–Smirnov test to estimate the normal distribution of raw data of genes related to ferroptosis. Mann–Whitney *U* test and an independent sample *t*-test were used for non-normal distribution data and normal distribution data, respectively. The statistical results are presented using Grand Prism 8 software.

Functional Enrichment and Protein-Protein Interaction Network

Gene Ontology (GO) is a widely utilized tool for annotating genes with their functions, particularly in the areas of molecular function (MF), biological processes (BP), and cellular components (CC). The Kyoto encyclopedia of genes and genomes (KEGG) enrichment analysis serves as a valuable practical resource for investigating gene functions and associated high-level genomic information. To gain a deeper understanding of the functions of differentially expressed genes (DEGs), functional enrichment analysis and a protein-protein interaction (PPI) network for the DEGs were established using Metascape (version: v3.5.20240101). Metascape is a web-based portal designed to provide comprehensive gene list annotation and analysis resources for experimental biologists. It is an effective and efficie t tool for researchers to analyze and interpret OMICs-based studies in the era of big data. This online tool includes modules such as enrichment clustering, protein network analysis, multi-gene list meta-analysis, and transcription factor analysis. Additionally, the cytoscape plug-in for molecular complex detection (MCODE) was employed to explore key functional modules within the PPI network.[19]

HIGHLIGHTS

- Based on network pharmacology, bioinformatics analysis, and molecular docking studies, we found that pulmonary artery hypertension (PAH) is associated with a series of abnormalities in downstream molecular signaling pathways, including DNA damage, immune dysregulation, vascular endothelial growth factor (VEGF) signal deficienc , and iron-induced apoptosis. Isorhamnetin emerges as a promising candidate compound for the treatment of PAH in these aspects.

Transcription Factor Analysis

Transcription regulatory relationships unraveled sentence-based text mining (TRRUST) (https://www.grnpedia.org/trrust/, version 2) is a manually curated database of transcriptional regulatory networks for humans and mice. This database includes 8444 and 6552 TF-target regulatory relationships of 800 human TFs and 828 mouse TFs, respectively. These relationships have been derived from 11237 PubMed articles that detail small-scale experimental studies on transcriptional regulation. To facilitate efficie t searches for regulatory relationships among over 20 million PubMed articles, the TRRUST database also provides information on the mode of regulation (activation or repression). Currently, 8972 (59.8%) of the regulatory relationships have a known mode of regulation.[20] In the results of GO and KEGG analyses, down-regulated genes were found to be enriched in functional pathways related to cellular responses to growth factor stimuli, responses to growth factors, and blood vessel development. Consequently, in this database, we searched for the TFs associated with VEGF-A, VEGF-B, and VEGF-C, which are well-studied core components of arterial endothelial growth factor signaling. The analysis was conducted using SPSS software (version 20.0). We used the Kolmogorov–Smirnov test to estimate the normal distribution of raw data of transcription factors (TFs). Mann–Whitney *U* test and an independent sample *t*-test were used for non-normal distribution data and normal distribution data, respectively. The statistical results are presented using Grand Prism 8 software.

Immune Filtration Analysis

ImmuCellAI (Immune Cell Abundance Identifier) is a tool designed to estimate the abundance of 24 immune cell types from gene expression datasets, including RNA-Seq and microarray data. These 24 immune cells comprise 18 T-cell subtypes and 6 additional immune cells: B cells, NK cells, monocyte cells, macrophage cells, neutrophil cells, and dendritic cells (DCs).[21,22]

In our study, we analyzed the immune infilt ation of PAH using a specialized tool. Additionally, we compared the expression levels of 10 immune checkpoint genes between PAH samples and control samples. Microarray data were downloaded from theGEO database (http://www.ncbi.nih.gov/geo) in MINiML format.[23-25] We extracted the expression data of immune checkpoint genes and examined the expression values of these genes. The analysis was conducted using SPSS software (version 20.0). We used the Kolmogorov–Smirnov test to estimate the normal distribution of raw data of immune checkpoint genes. Mann–-Whitney *U* test and an independent sample *t*-test were used for non-normal distribution data and normal distribution data, respectively. The statistical results are presented using Grand Prism 8 software.

Isorhamnetin Targets

Comparative toxicogenomics database (CTD) is a comprehensive, publicly accessible database designed to enhance our understanding of how environmental exposures affect human health. It offers meticulously curated information on chemical-gene/protein interactions, chemical-disease relationships, and gene-disease associations. This data is integrated with functional and pathway information to support the development of hypotheses regarding the mechanisms underlying diseases influen ed by environmental factors. In this study, we utilized CTD to identify the targets of Isorhamnetin.[26]

Molecular Docking

NFE2L2 was identified as a common gene among DEGs, ferroptosis, and isorhamnetin, those interacting with isorhamnetin. Consequently, we conducted molecular docking to assess the binding affinities between isorhamnetin and NFE2L2. The crystal structures of the Nrf2/NFE2L2, VEGFR, ZNF24, and ATM proteins used for docking were obtained from the protein data bank (PDB), which is accessible at https://www.rcsb.org/.The PDB IDs for the 4 proteins are 7X5E 1FLT, 3LHR, and 7SIC, respectively.[27-30]

The 3-dimensional (3D) structure of the small molecule isorhamnetin was downloaded from the PubChem database (PubChem CID: 5281654), and energy minimization was performed using the MMFF94 force field. AutoDock Vina 1.2.3 software, developed by the Scripps Research Institute, was utilized for molecular docking. Prior to docking, PyMol 2.5.5 was employed to remove water molecules, salt ions, and small molecules.[31] The coordinates for docking are listed in Table 1. Additionally, we used ADFRsuite 1.03 to convert all processed small molecules and receptor proteins into the PDBQT format for docking with AutoDock Vina 1.2.3 docking.[32] During the docking process, the global search granularity was set to 32, while all other parameters were maintained at their default settings. The docking conformation with the highest output score was considered the binding conformation, and the docking results were visualized using PyMOL 2.5.5.

Estimating Toxify Profil s of Isorhamnetin

ADMETlab 3.0 (available at: https://admetlab3.scbdd.com/server/evaluation) is the second updated version of the web server that offers a comprehensive and efficie t platform for evaluating ADMET-related parameters, physicochemical properties, and medicinal chemistry characteristics involved in the drug discovery process.[33] In our study, we assessed the toxicity profiles of isorhamnetin using ADMETlab (version 3.0). The imported SMILES representation of isorhamnetin is as follows: COC1=C(C=CC(=C1)C2=C(C(=O)C3=C(C=C(C=C3O2)O)O)O)O or O1C2=C([H])C(=C([H])C(=C2C(C(=C1C1C([H])=C([H])C(=C(C=1[H])OC([H])([H])[H])O[H])O[H])=O)O[H])O[H].

Statement

We do not use artificial intelligence (AI) assistive technologies (such as large language models (LLMs), chatbots, or image creators).

The study is secondary and has no ethical implications.

RESULTS

Identifi ation of DEGs in PAH

Figure 1 illustrates the workfl w chart. The microarray dataset GSE113439 was obtained from the GEO database. An

Table 1. Ferroptosis Genes Expression Between PAH Group and Control Group

	PAH group (n = 15)			Control group (n = 11)			Kolmogorov–Smirnova test	Independent Samples Test		Mann–Whitney *U* test
Genes	**n**	**Mean**	**Std. Error**	**n**	**Mean**	**Std. Error**	***P***	***T* value**	***P* (2-tailed)**	***P***
ACSL4	15	9.776	0.105	11	8.706	0.175	.173	5.55	< .001	
ALOX15	15	8.090	0.301	11	8.116	0.236	.172	−0.063	.950	
ATP5MC3	15	7.065	0.044	11	7.106	0.035	.200	−0.675	.506	
CARS	15	8.223	0.079	11	7.873	0.091	.200	2.902	.008	
CDKN1A	15	9.746	0.164	11	10.073	0.188	.200	−1.306	.204	
CISD1	15	8.704	0.098	11	8.828	0.086	.200	−0.907	.374	
DPP4	15	9.892	0.125	11	8.389	0.150	.200	7.743	< .001	
FANCD2	15	6.679	0.124	11	5.991	0.057	.154	4.466	< .001	
FDFT1	15	11.221	0.066	11	11.137	0.105	.078	0.714	.482	
GLS2	15	6.845	0.038	11	6.887	0.043	.200	−0.722	.477	
GPX4	15	11.433	0.058	11	11.763	0.060	.200	−3.887	.001	
HSPA5	15	11.880	0.090	11	10.913	0.105	.200	7.004	< .001	
HSPB1	15	12.653	0.045	11	12.865	0.046	.200	−3.218	.004	
LPCAT3	15	11.326	0.069	11	11.727	0.070	.200	−4.021	< .001	
MT1G	15	12.026	0.163	11	11.845	0.169	.200	0.754	.458	
NCOA4	15	10.606	0.049	11	9.885	0.114	.065	5.805	< .001	
NFE2L2	15	10.909	0.057	11	10.141	0.097	.200	7.229	< .001	
RPL8	15	13.035	0.021	11	13.087	0.031	.200	−1.423	.168	
SAT1	15	12.417	0.062	11	12.199	0.085	.200	2.134	.043	
SLC1A5	15	9.700	0.101	11	10.007	0.097	.200	−2.128	.044	
SLC7A11		8.460	0.306	11	6.105	0.126	.135	7.125	< .001	
TFRC	15	10.808	0.127	11	9.890	0.158	.200	4.586	< .001	
CS	15	10.785	0.058	11	10.630	0.021	.006	2.197	< .001	.038
EMC2	15	9.310	0.058	11	8.706	0.095	.043	5.713	< .001	< .001

Pulmonary arterial hypertension (PAH) group (n = 15): GSM3106326, GSM3106327, GSM3106328, GSM3106329, GSM3106330, GSM3106331, GSM3106332, GSM3106333, GSM3106334, GSM3106335, GSM3106336, GSM3106337, GSM3106338, GSM3106339, GSM3106340; Control group (n = 11): GSM3106341, GSM3106342, GSM3106343, GSM3106344, GSM3106345, GSM3106346, GSM3106347, GSM3106348, GSM3106349, GSM3106350, GSM3106351. PAH, pulmonary arterial hypertension.

adjusted *P*-value threshold of less than .05 and a |log2FC| of 1.5 or greater were applied. Consequently, 22 841 genes were included in the analysis. We identified a total of 2604 DEGs, comprising 1962 upregulated genes and 642 downregulated genes. The results were visualized using volcano plots (Figure 2A and B).

Enrichment ofDEGs and establishment ofPPI network

To investigate the biological functions of these DEGs,GO andKEGG pathway enrichment analyses were conducted on 1962 upregulated genes and 642 downregulated genes associated with PAH, utilizing the Metascape online tool. The results revealed that the top functional GO terms for upregulated DEGs included the mitotic cell cycle and DNA damage response, while the downregulated DEGs were primarily associated with vasculature development and cellular responses to growth factor stimuli (Figure 2C, E). The leading KEGG pathways identified were herpes simplex virus 1 infection for upregulated genes and pathways in cancer for downregulated genes (Figure 2D, F). Additionally, the MCODE plug-in was employed to explore signifi ant gene clustering modules. The findings indicated that DNA damage response, mitotic cell cycle, and chromosome organization were enriched in upregulated genes, whereas cellular responses to growth factor stimuli, responses to growth factors, and blood vessel development were enriched in downregulated genes. These results, illustrated in Figure 3, suggest that cell proliferation and DNA damage play a signifi ant role in the molecular pathology of PAH, alongside a reduction in vascular VEGF signaling.

Differentially Expressed Genes of Ferroptosis-Related Genes

Twenty-four ferroptosis-related genes were identified and analyzed. The results indicate that genes associated with ferroptosis, such as *ACSL4, CARS, CS, DPP4, EMC2, FANCD2, HSPA5, NCOA4, NFE2L2, SLC7A11, SAT1,* and *TFRC*, were signifi antly upregulated in 15 samples of PAH. In contrast, *GPX4, HSPB1, SLC1a5* and *LPCAT3* were signifi antly downregulated. These findings suggest that the ferroptosis process may play a role in the pathology of PAH. The results are illustrated in Figure 4 and Table 1.

Transcription Factors

The results of the KEGG analysis and MCODE estimation indicated that the cellular response to growth factor

stimulus, response to growth factor, and blood vessel development were the top pathways affected in the down-regulated genes associated with PAH. It is well established that VEGF signaling plays a crucial role in blood vessel activities. These findings suggest a potential reduction in VEGF signaling. Consequently, we investigated theTFs regulating the expression of VEGF-A, VEGF-B, and VEGF-C by consulting the TRRUSS database. We identified 58 TFs for VEGF-A, 7 TFs for VEGF-B, and 2 TFs for VEGF-C, as presented in Figure 5A. Among the TFs for VEGF-A, 6 common TFs (*RB1, HDAC2, HIF1A, ZNF24, ATM, MEF2C*) were found in the up-regulatedDEGs, while 1 TF (ID3) was identified in the down-regulated DEGs. In contrast, only 1 common TF *(HIF1A*) was identified for VEGF-B among the DEGs. No common TFs were found between the DEGs and TFs for VEGF-C. These results are displayed in Figure 5B. The differentially expressed TFs showed statistical signifi ance between the PAH samples and control samples, as illustrated in Figure 5C and Table 2.

Immune Characteristics in Pulmonary Arterial Hypertension

The raw microarray data of PAH were input into the immune cell abundance identifie . The results indicated that the distribution and infilt ation of immune cells in PAH samples were altered compared to control samples. The affected immune cells included dendritic cells (DC), macrophages, natural killer (NK) cells, neutrophils, CD8+ T cells, infla - matory Helper T 17 cells, T follicular helper (Tfh) cells, cytotoxic T cells, central memory T cells, and effector memory T cells. The infilt ation score slightly increased in PAH samples (0.866) compared to control samples (0.837) (*P* = .02). These results are illustrated in Figure 6 and Table 3. Additionally, 8 immune checkpoint genes were signifi antly expressed, with 4 highly expressed genes (*CD274, HAVCR2, PDCD1LG2*) and 4 lowly expressed genes (*IGSF8, LAG3, SIGLEC15, TIGIT*) compared to the control. These findings are presented in Figure 7 and Table 4. Overall, these results suggest that the pathology of PAH is associated with immune responses and inflammation

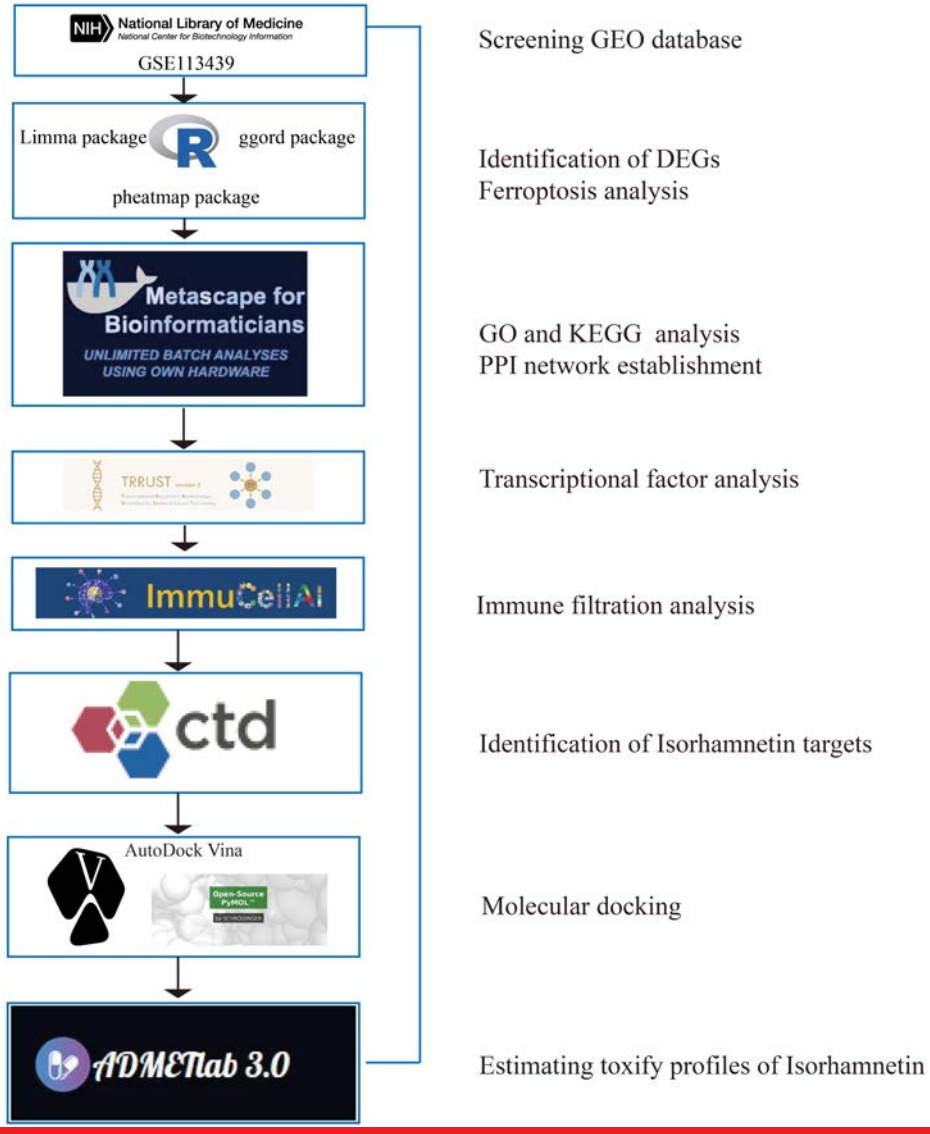

Figure 1. Work fl wchart.

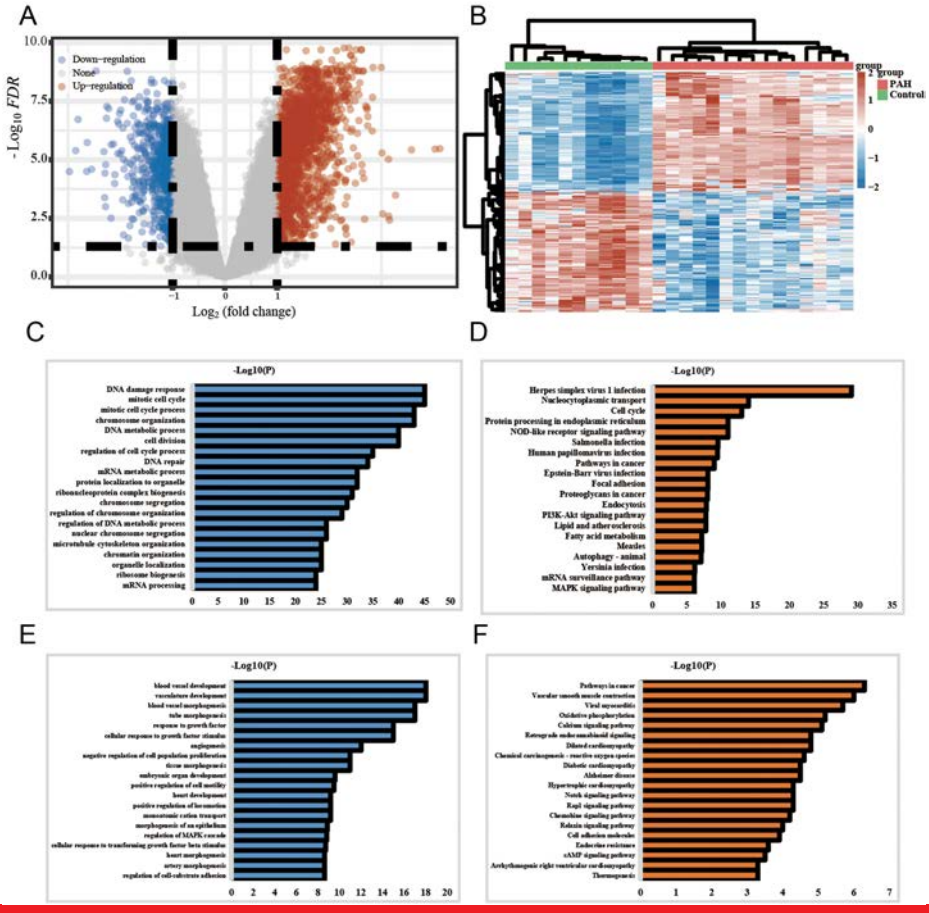

Figure 2. Analysis of GSE113439. (A) Volcano plot of DEGs between the PAH samples and control samples. (B) Heatmap of DEGs between the PAH samples and control samples. (C, D) Gene ontology and KEGG analysis of upregulated genes, the data were presented as Log_2(fold change). (E, F) Gene ontology and KEGG analysis of downregulated genes, the data were presented as—Log10 (*P* value).

Identifi ation of Isorhamnetin

We extracted 58 isorhamnetin-interacting genes from theCTD. These genes are highly enriched in various biological processes, including responses to hormones, response to xenobiotic stimuli, response to oxidative stress, inorganic substances, peptides, and chemical stress. Additionally, they are involved in the regulation of inflamma ory responses, responses to molecules of bacterial origin, toxic substances, and lipopolysaccharides (Figure 8A, D, E). The most enriched pathways include the AGE-RAGE signaling pathway in diabetic complications, pathways in cancer, lipid metabolism and atherosclerosis, fluid shear stress and atherosclerosis, Chagas disease, toxoplasmosis, chemical carcinogenesis involving reactive oxygen species, diabetic cardiomyopathy, Th17 cell differentiation, and hepatitis B (Figure 8B, C, E). Furthermore, 2604 DEGs, 24 ferroptosis-related genes, and 58 isorhamnetin targets identified through various algorithms were intersected using Venn diagram analysis. One interacting gene, NFE2L2, was identified among the DEGs, DEGs related to ferroptosis, and the targets of isorhamnetin. We consider that NFE2L2 contributes to the pathological mechanism of PAH related to ferroptosis. Additionally, NFE2L2 may serve as a potential therapeutic target for isorhamnetin in the treatment of PAH. The results are illustrated in Figure 9A and B.

Binding Capacity of Isorhamnetin to NFE2L2, VEGFR, ATM, and ZNF24

Molecular docking simulation technology is a convenient and effective method for exploring the interactions between small molecules and target proteins. Therefore, we utilized Vina 1.2.3 software to estimate the binding affinity of isorhamnetin to NFE2L2, VEGFR, ZNF24, and ATM. The results of the molecular docking indicate that chemical-protein interactions with a docking energy of less than 5 kcal/mol suggest a strong binding affinit .[34]

Isorhamnetin forms hydrogen-bonding interactions with NFE2L2 at specific amino acid sites, including PHE-490, ARG-499, ASN-482, and MET-485. The establishment of these hydrogen bonds enhances the binding affinity between proteins and small molecules. Additionally, Isorhamnetin exhibits hydrophobic interactions with NFE2L2 at the amino acid site MET-485, which may contribute to strong van der Waals forces between the molecules. The calculated affinity score of −6.869 kcal/mol between isorhamnetin and NFE2L2 indicates a favorable binding capacity of Isorhamnetin to NFE2L2 (Figure 9C and Table 5). Isorhamnetin forms hydrogen-bonding interactions with VEGFR at specific amino acid sites, including CYS-68, GLY-59, and GLN-37. Furthermore, isorhamnetin also forms hydrophobic interactions with VEGFR at the amino acid

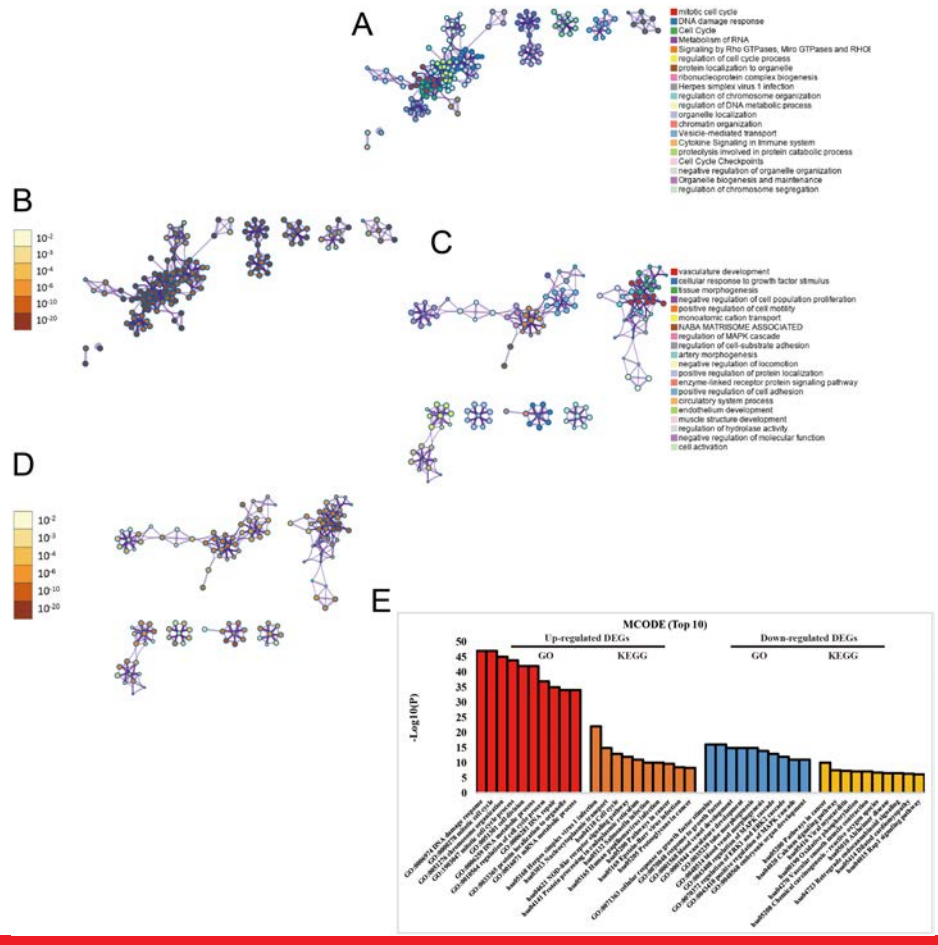

Figure 3. Protein-protein interaction network of enriched terms with MCODE plug-in estimation. (A) Protein-protein interaction network of up-regulated genes, colored by cluster ID, where nodes that share the same cluster ID are typically close to each other. (B) Protein-protein interaction network of up-regulated genes, colored by *P*-value, where terms containing more genes tend to have a more signifi ant *P*-value. (C) Protein-protein interaction network of down-regulated genes, where nodes that share the same cluster ID are typically close to each other. (D) Protein-protein interaction network of down-regulated genes, colored by *P*-value, where terms containing more genes tend to have a more signifi ant *P*-value. (E) MCODE estimation (Top 10).

sites THR-31 and ARG-56, with a binding energy of –6.508 kcal/mol (Figure 9D and Table 2). For ZNF24, isorhamnetin forms hydrophobic interactions at amino acid sites, including LEU-84, PHE-57, LEU-65, LEU-87, and LEU-61 (–6.882 kcal/mol) (Figure 9E and Table 5). Isorhamnetin forms hydrogen-bonding interactions with ATM at several amino acid sites, including CYS-2770, THR-2773, and LYS-2717. Isorhamnetin also forms hydrophobic interactions with ATM at the amino acid sites LEU-2877, TRP-2769, LEU-2767, PRO-2699, and LEU-2715, with a binding energy of –7.878 kcal/mol (Figure 9 F and Table 2).

Toxicity Prediction of Isorhamnetin

We conducted ADMET predictions using ADMETlab 3.0 and found no acute toxicity associated with the oral administration of isorhamnetin. While there is no validated evidence of carcinogenicity, skin sensitization was identified (see Table 6). These results suggest that the oral administration of isorhamnetin is safe.

DISCUSSION

Pulmonary arterial hypertension, a well-studied form of pulmonary hypertension, is classified as pre-capillary pulmonary hypertension. Advances in genetics and molecular medicine have led to the identifi ation of genetic variations and susceptibilities associated with the onset of PAH. Factors such as genetic mutagenesis, DNA damage and repair, and the activation of cell death pathways contribute to the pathological processes underlying PAH. The most extensively studied mutated gene is BMPR2. In Western populations, 70% to 80% of patients with hereditary PAH and 10% to 20% of patients with idiopathic PAH (IPAH) have been found to carry mutations in the BMPR2 gene. These mutations are associated with early onset, severe clinical phenotypes, and poor outcomes. Although the exact causes and mechanisms of PAH remain unclear, it is generally accepted that multiple factors, pathways, and processes are involved. Currently, molecularly targeted therapies such as ambrisentan and tadalafil are employed to improve clinical conditions or exercise tolerance. However, there are still no effective drugs available to delay disease progression. Therapeutic interventions for PAH primarily focus on managing pathophysiological processes and controlling complications associated with the

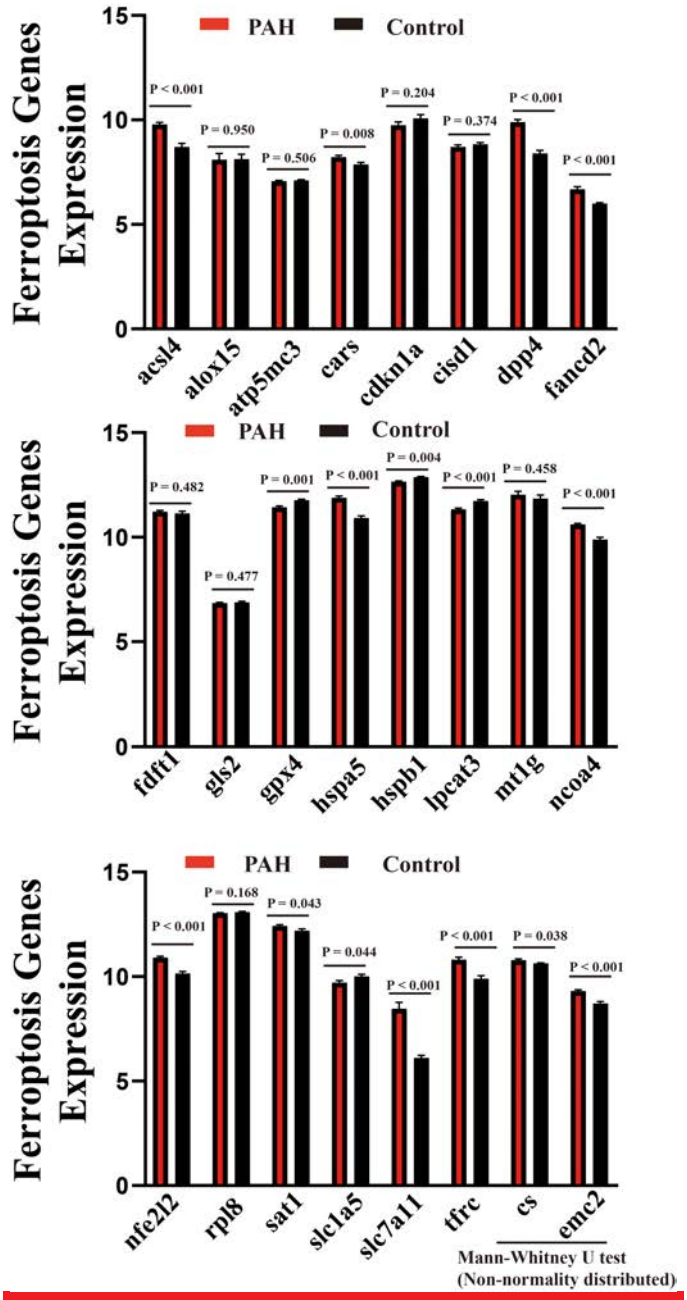

Figure 4. Identifi ation of ferroptosis related genes with Wilcox test between PAH samples and control samples.

condition. Therefore, identifying key regulatory genes and functional pathways is essential.

In this study, we utilized GSE113439 to analyze the DEGs associated with PAH. We identified highly expressed genes in PAH samples that were signifi antly enriched in biological pathways related to DNA damage response, the mitotic cell cycle, and chromosome organization. Additionally, we observed notable changes in the expression levels of genes associated with ferroptosis. These findings suggest an activation of cell death pathways, cell protection mechanisms, and cell cycle progression in the development of PAH. Conversely, downregulated genes were signifi antly enriched in pathways associated with cellular responses to growth factor stimuli, responses to growth factors, and blood vessel development. It is well known that pulmonary artery endothelial cell (PAEC) dysfunction is the most common inducer of the occurrence and progression of PAH, and that VEGF signaling contributes to these functional processes.[35] Chakraborty et al[35] discovered that the loss of microvessels and the reduction ofVEGF-induced tip cell formation were crucial mechanisms in PAH.[36] We interpreted the enrichment results of downregulated genes as indicating a decrease in vascular VEGF signaling. Consequently, we conducted a search forTFs that regulate VEGF-A, B, and C, identifying 7 common TFs with validated functions that overlapped with DEGs. Among these common TFs, ATM and ZNF24 are involved in repressing VEGF-A transcription. These 2 genes could potentially serve as targets for modulating reduced VEGF signaling.

Recent studies have confirmed that patients with PAH exhibit iron metabolic abnormalities, which are correlated with a decline in athletic performance, decreased survival rates, and the worsening of clinical symptoms.[5,37] Ferroptosis is precisely regulated at multiple levels, including the epigenetic, transcriptional, and post-transcriptional levels. Zhang and colleagues identified 8 ferroptosis-related genes in lung tissue from patients with PAH, which included 4 driver genes (IDH1, DPP4, HIF1A, ACSL4) and 3 suppressor genes (SLC7A11, HIF1A, PLIN2). Their results indicated that both promoting and inhibiting factors coexisted in the progression of ferroptosis.[5] In our study, we identified 24 ferroptosis-related genes. Eleven genes (ACSL4, CARS, CS, DPP4, EMC2, FANCD2, HSPA5, NCOA4, NFE2L2, SLC7A11, and TFRC) were signifi antly upregulated in 15 PAH samples compared to the control samples, while GPX4, HSPB1, LPCAT3, and RPL8 were signifi antly downregulated. The results of the independent comparison of ferroptosis-related genes between the PAH samples and control samples differed from those obtained through the DEGs screening. The signifi ance of the comparison results between the 2 sample groups was assessed using the Wilcoxon test, whereas in the DEGs screening process, we established a threshold of |Log2 (Fold Change)| > 1.5. Importantly, NFE2L2 has been identified as the central regulatory target of isorhamnetin, ferroptosis, and DEGs associated with PAH. The complex alterations in cytokine activation, inflammation, cellular immunity, and autoantibody responses suggest that PAH is, in part, an autoimmune and inflamma ory disease.[13,38] In the current study, we performed an immune infilt ation analysis and assessed the expression levels of immune checkpoints. We observed a signifi ant increase in the immune infilt ation score in PAH samples compared to control samples. Furthermore, there were notable changes in the expression levels of immune checkpoints. The dysregulation of these immune checkpoints indicates abnormal immune responses and contributes to the pathophysiology of PAH.

Isorhamnetin (3-methylquercetin) is a natural compound that belongs to the class of 3-O-methylated metabolites of quercetin. Isorhamnetin demonstrates both preventive and therapeutic effects on cardiovascular and cerebrovascular diseases, including anti-atherosclerotic properties, protection of endothelial cells, anti-myocardial ischemia effects,

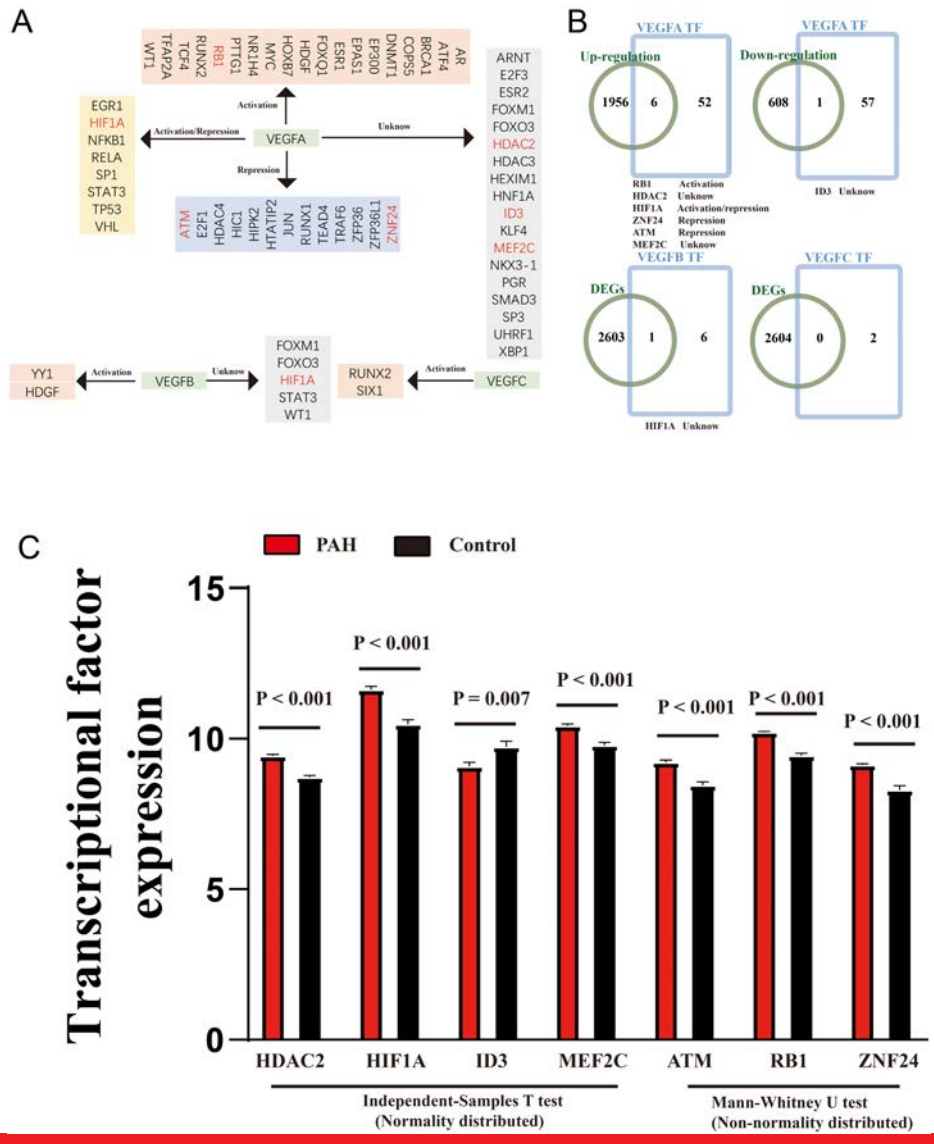

Figure 5. Transcriptional factor analysis of VEGFs. (A) TFs for VEGFs regulation. (B) Intersection of TFs and DEGs. (C) Transcriptional factor analysis with Wilcox test between PAH samples and control samples.

Table 2. Transcriptional Factor Expression between PAH Group and Control Group

	PAH Group (n = 15)			Control Group (n = 11)			Kolmogorov–Smirnova test	Independent Samples test		Mann–Whitney *U* test
Genes	**n**	**Mean**	**Std. Error**	**n**	**Mean**	**Std. Error**	***P***	***T* value**	***P* (2-tailed)**	***P***
HDAC2	15	9.425	0.059	11	8.724	0.059	.130	8.147	< .001	
HIF1A	15	11.628	0.111	11	10.477	0.155	.200	6.205	< .001	
ID3	15	9.079	0.136	11	9.736	0.179	.200	−2.974	.007	
MEF2C	15	10.426	0.062	11	9.776	0.109	.200	5.516	< .001	
ATM	15	9.222	0.077	11	8.459	0.105	.040	5.986	< .001	< .001
RB1	15	10.213	0.034	11	9.446	0.074	.009	9.466	< .001	< .001
ZNF24	15	9.128	0.039	11	8.300	0.146	< .001	5.493	< .001	< .001

Pulmonary arterial hypertension (PAH) group (n = 15): GSM3106326, GSM3106327, GSM3106328, GSM3106329, GSM3106330, GSM3106331, GSM3106332, GSM3106333, GSM3106334, GSM3106335, GSM3106336, GSM3106337, GSM3106338, GSM3106339, GSM3106340; Control group (n = 11): GSM3106341, GSM3106342, GSM3106343, GSM3106344, GSM3106345, GSM3106346, GSM3106347, GSM3106348, GSM3106349, GSM3106350, GSM3106351. PAH, pulmonary arterial hypertension.

anti-hypotension actions, anti-hypoglycemic effects, and anti-thrombotic properties, among others.[13] The mechanisms underlying these beneficial effects are associated with its antioxidant, anti-inflamma ory, and anti-mitoc hondrial-dependent effects on cell apoptosis.[10-15] REN et al[14] found that isorhamnetin signifi antly improved outcomes in acute lung injury, asthma, and non-small cell lung cancer. Isorhamnetin can suppress the production of reactive oxygen species (ROS), mitochondrial arachidonic acid (AA) and iron-induced dysfunction, as well as glutathione (GSH) reduction. In our study, we identified 58 target genes that interact with isorhamnetin. These target genes intersected with DEGs associated with PAH, ferroptosis-related genes, and the transcription factor NFE2L2. NFE2L2 was initially recognized as a crucial regulator of redox homeostasis in cells. Subsequent research has revealed that NFE2L2 is also responsible for maintaining protein homeostasis, regulating the pentose phosphate pathway, and facilitating amino acid and carbohydrate metabolism.[39-42]

Previous studies have indicated that NFE2L2 plays a crucial role in enhancing the body's defense against ferroptosis. NFE2L2 regulates iron balance and the ferroptosis process through HERC2, VAMP8, and NCOA4. Elevated levels of NFE2L2 amplify its effects.[43] Consequently, we conducted molecular docking studies to investigate the binding capabilities of isorhamnetin to NFE2L2 and other transcription factors (VEGFR, ATM, and ZNF24) associated with VEGF signaling. Our findings revealed that isorhamnetin exhibited strong affinities for these crucial regulators of PAH. These results suggest that isorhamnetin could be a promising natural compound in the fig t against PAH.

CONCLUSION

Based on the results of the current analysis, we found that PAH is characterized by a series of abnormalities in downstream molecular signaling pathways, including DNA damage, immune dysregulation, VEGF signaling deficienc , and the ferroptosis process. These factors may be the core pathophysiological mechanisms of PAH. Ferroptosis-related genes, such as NFE2L2 and TF (including ATM and ZNF24) associated with VEGF signaling, serve as potential candidate therapeutic targets that contribute to the mechanisms mentioned above. Isorhamnetin is identified as a candidate compound for the treatment of PAH.

Statements and Declarations: The authors declare that they have no potential conflicts of interests. Study design: Yangliu; Data analysis and presentation: Chenshao, Weixia, and Yangliu; Writing and revision: Chenshao, Weixia, and Yangliu; Supervision: Yangliu. All authors contributed equally to this work.

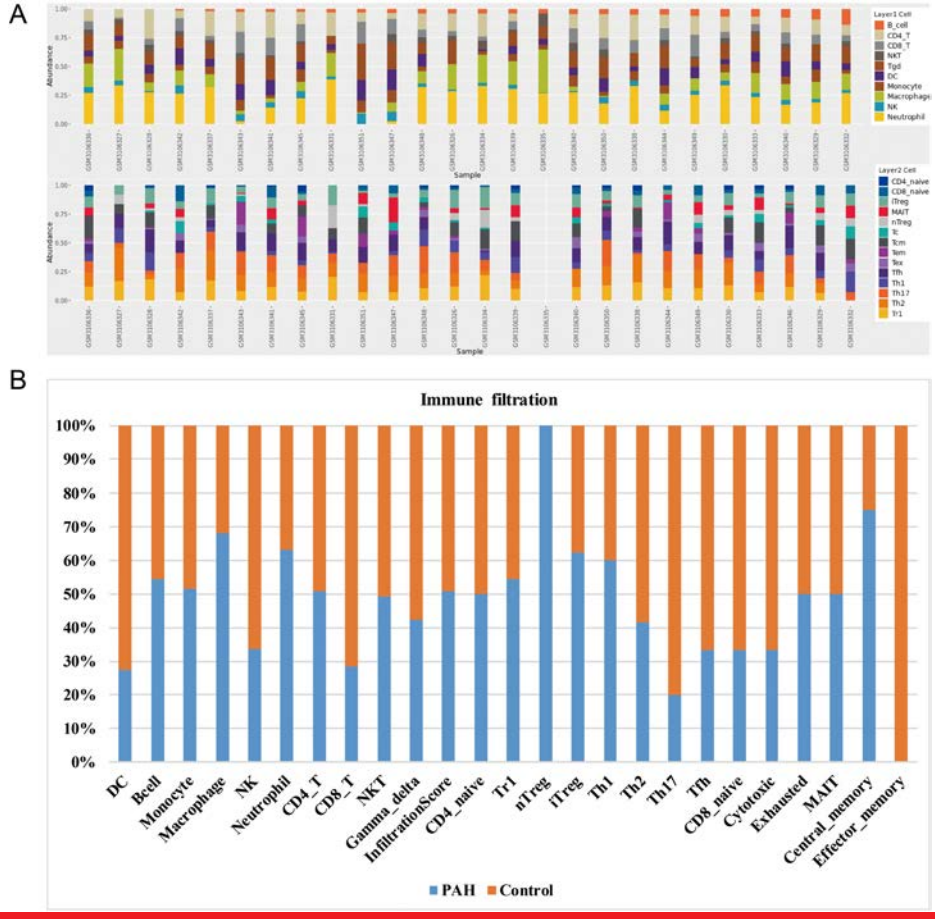

Figure 6. Immune filt ation analysis. (A) Immune cell abundance in sample (B) Immune cell abundance in groups.

Table 3. Immune Filtration Analysis between PAH Group and Control Group

Immune Cells	PAH Group (n = 15)	Control Group (n = 11)	*P*
Dendritic cell	0.05	0.132	< .001
Bcell	0.042	0.035	.720
Monocyte	0.068	0.064	.980
Macrophage	0.175	0.082	.011
NK	0.028	0.055	< .001
Neutrophil	0.286	0.167	< .001
CD4_T	0.131	0.127	.940
CD8_T	0.051	0.128	< .001
Natural killer T cell	0.039	0.040	.900
Gamma_delta	0.130	0.176	.069
CD4_naive	0.001	0.001	1.000
Tr1	0.006	0.005	.700
Natural regulatory T cell	0.002	0.000	.066
Induced regulatory T cell	0.005	0.003	.120
Th1	0.003	0.002	.140
Th2	0.005	0.007	.140
Th17	0.002	0.008	< .001
Tfh	0.004	0.008	.022
CD8_naive	0.001	0.002	.150
Cytotoxic	0.001	0.002	.016
Exhausted	0.001	0.001	.830
Mucosal-associated invariant T cell	0.002	0.002	.330
Central_memory	0.006	0.002	.004
Effector_memory	0.000	0.004	.001
Infilt ation score	0.866	0.837	.020

Pulmonary arterial hypertension (PAH) group (n = 15): GSM3106326, GSM3106327, GSM3106328, GSM3106329, GSM3106330, GSM3106331, GSM3106332, GSM3106333, GSM3106334, GSM3106335, GSM3106336, GSM3106337, GSM3106338, GSM3106339, GSM3106340; Control group (n = 11): GSM3106341, GSM3106342, GSM3106343, GSM3106344, GSM3106345, GSM3106346, GSM3106347, GSM3106348, GSM3106349, GSM3106350, GSM3106351. NK, natural killer; PAH, pulmonary arterial hypertension; Tfh, T follicular helper

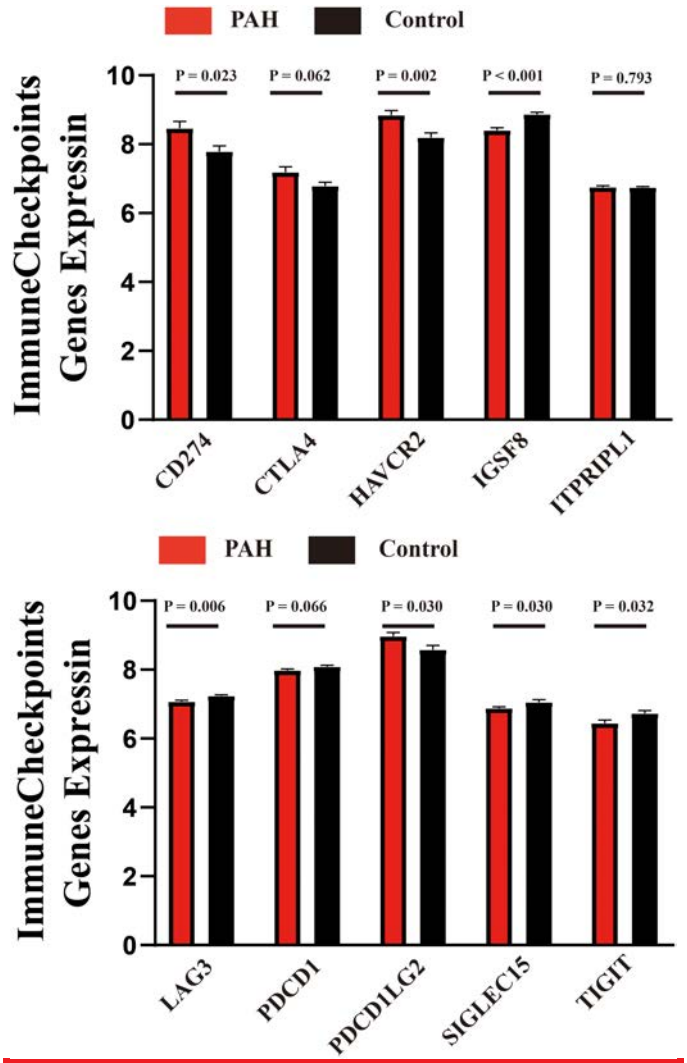

Figure 7. Comparison of expression levels of immune checkpoint genes between PAH samples (n = 15) and control samples (n = 11).

Table 4. Immune Checkpoint Expression between PAH Group and Control Group

	PAH Group (n = 15)			Control Group (n = 11)			Kolmogorov–Smirnova Test	Independent Samples Test	
Genes	**n**	**Mean**	**Std. Error**	**n**	**Mean**	**Std. Error**	***P***	***T* value**	***P* (2-tailed)**
CD274	15	8.462	0.203	11	7.790	0.167	.20	2.425	.023
CTLA4	15	7.191	0.157	11	6.786	0.110	.19	1.959	.062
HAVCR2	15	8.849	0.128	11	8.194	0.137	.20	3.437	.002
IGSF8	15	8.406	0.076	11	8.873	0.050	.06	−4.566	.000
ITPRIPL1	15	6.756	0.037	11	6.742	0.031	.20	0.265	.793
LAG3	15	7.071	0.042	11	7.241	0.033	.20	−2.999	.006
PDCD1	15	7.976	0.042	11	8.089	0.037	.20	−1.926	.066
PDCD1LG2	15	8.969	0.111	11	8.582	0.123	.20	2.306	.030
SIGLEC15	15	6.882	0.041	11	7.057	0.069	.20	−2.3	.030
TIGIT	15	6.448	0.088	11	6.732	0.083	.08	−2.28	.032

Pulmonary arterial hypertension (PAH) group (n = 15): GSM3106326, GSM3106327, GSM3106328, GSM3106329, GSM3106330, GSM3106331, GSM3106332, GSM3106333, GSM3106334, GSM3106335, GSM3106336, GSM3106337, GSM3106338, GSM3106339, GSM3106340; Control group (n = 11): GSM3106341, GSM3106342, GSM3106343, GSM3106344, GSM3106345, GSM3106346, GSM3106347, GSM3106348, GSM3106349, GSM3106350, GSM3106351. PAH, pulmonary arterial hypertension.

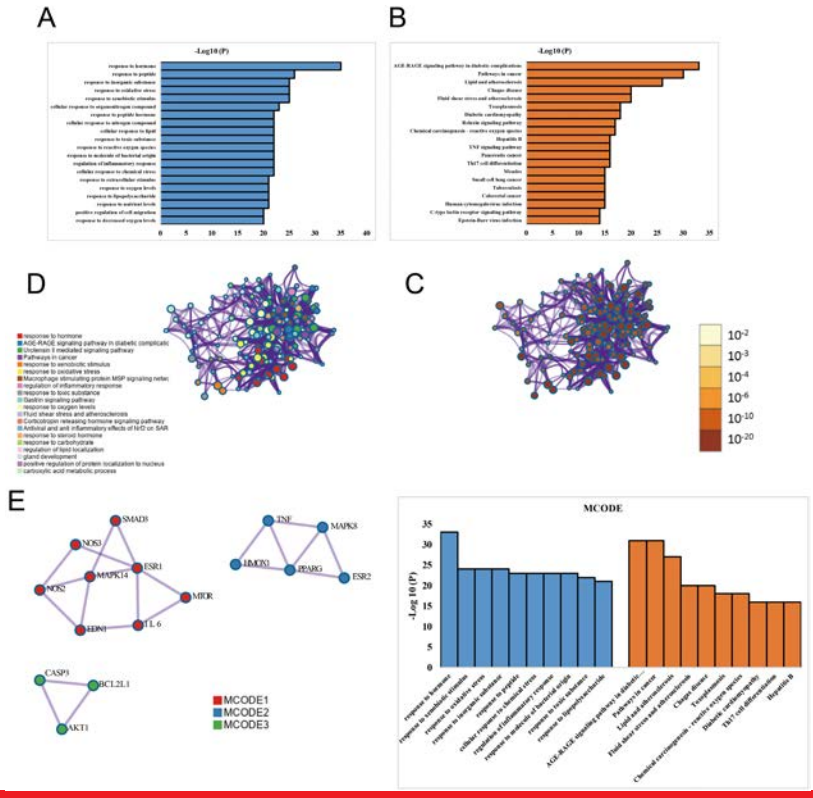

Figure 8. Functional enrichments of isorhamnetin targets. (A, B) Gene oncology and KEGG pathway analyses. (C, D) Protein-protein interaction functional network analysis, color by cluster and *P*-value respectively. (E) Molecular Complex Detection estimation. Blue color denotes GO analysis and orange color denotes KEGG analysis.

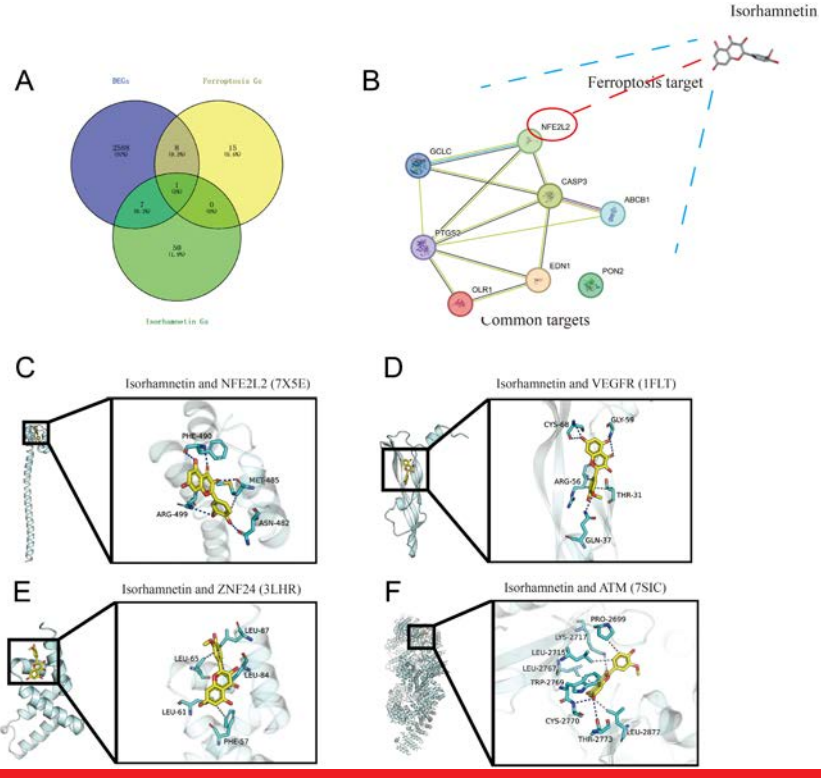

Figure 9. Molecular docking of isorhamnetin and identified common genes. (A) Identifi ation of intersecting genes of isorhamnetin targets, DEGs, and ferroptosis-related genes. (B) Interaction of isorhamnetin targets. (C-F) Binding capacity of isorhamnetin and predicted hub regulatory targets, including *NFE2L2 (PDB ID: 7X5E), VEGFR (PDB ID: 1FLT), ZNF24 (PDB ID: 3LHR),* and *ATM (PDB ID: 7SIC*).

Table 5. Molecular Docking of the Interaction of Isorhamnetin and Target Genes

Targets	PDB ID	Chemical	Coordinate	Grid Size	Docking Score (kcal/mol)	Hydrophobic Interactions	Hydrogen Bonds
Nrf2/NFE2L2	7X5E	Isorhamnetin	x = −59.12, y = −18.90, z = 4.03	x = 60, y = 60, z = 60	−6.869	MET-485	PHE-490, MET-485, ASN-482, ARG-499
VEGFR	1FLT	Isorhamnetin	x = −1.41, y = 7.71, z = 14.51	x = 20, y = 20, z = 20	−6.508	THR-31, ARG-56	CYS-68, GLY-59, GLN-37
ZNF24	3LHR	Isorhamnetin	x = 4.485, y = 32.47, z = 12.05	x = 45, y = 45, z = 45	−6.882	LEU-84, PHE-57, LEU-65, LEU-87, LEU-61	
ATM	7SIC	Isorhamnetin	x = 120.83, y = 166.20, z = 93.39	x = 20, y = 20, z = 20	−7.878	LEU-2877, TRP-2769, LEU-2767, PRO-2699, LEU-2715	CYS-2770, THR-2773, LYS-2717

PDB, protein data bank.

Table 6. Toxicophore Rules

Property	Value	Comment
Acute toxicity rule	0	20 substructures; acute toxicity during oral administration
Genotoxic carcinogenicity rule	0	117 substructures;carcinogenicity or mutagenicity
Nongenotoxic carcinogenicity rule	0	23 substructures; carcinogenicity through nongenotoxic mechanisms
Skin sensitization rule	8 alerts	155 substructures; skin irritation
Aquatic toxicity rule	0	99 substructures; toxicity to liquid (water)
Nonbiodegradable rule	1 alerts	19 substructures; non-biodegradable
SureChEMBL rule	0	164 substructures; MedChem unfriendly status
Toxicophores rule	1 alerts	154 toxic substructures from FAF-Drug 4

Ethics Committee Approval: Not applicable. All original materials can be obtained from the PubMed database (GSE113439) and corresponding study (Mura et al[16], Respirology 2019;24(11):1104-1110).

Peer-review: Internally peer reviewed.

Acknowledgments: We thank the providers of the protein structures in the PDB database (Sengoku et al[28], Wiesmann et al[27], Volkman et al., and Warren et al[30]), and to the providers of the microarray of PAH in the GEO database (Mura et al[16]).

Author Contributions: Concept – Y.L., C.S.; Design – Y.L.; Supervision – Y.L.; Resources – W.X., C.S., Y.L.; Materials – W.X., C.S., Y.L.; Data Collection and/or Processing – W.X., C.S., Y.L.; Analysis and/or Interpretation – W.X., C.S., Y.L.; Literature Search – W.X., C.S., Y.L.; Writing – W.X., C.S., Y.L.; Critical Review – C.S., Y.L.

Declaration of Interests: The authors have no conflict of interest to declare.

Funding: The authors declared that this study has received no financial support.

REFERENCES

1. Humbert M, Kovacs G, Hoeper MM, et al. 2022 ESC/ERS Guidelines for the diagnosis and treatment of pulmonary hypertension. *Eur Respir J*. 2023;61(1):1-144. [CrossRef]
2. Omura J, Habbout K, Shimauchi T, et al. Identifi ation of long noncoding RNA H19 as a new biomarker and therapeutic target in right ventricular failure in pulmonary arterial hypertension. *Circulation*. 2020;142(15):1464-1484. [CrossRef]
3. Sumneang N, Siri-Angkul N, Kumfu S, Chattipakorn SC, Chattipakorn N. The effects of iron overload on mitochondrial function, mitochondrial dynamics, and ferroptosis in cardiomyocytes. *Arch Biochem Biophys*. 2020;680:108241. [CrossRef]
4. Zou HX, Qiu BQ, Lai SQ, et al. Iron metabolism and idiopathic pulmonary arterial hypertension: new insights from bioinformatic analysis. *BioMed Res Int*. 2021;2021:5669412. [CrossRef]
5. Zhang F, Liu H. Identifi ation of ferroptosis-associated genes exhibiting altered expression in pulmonary arterial hypertension. *Math Biosci Eng*. 2021;18(6):7619-7630. [CrossRef]
6. Miyamoto HD, Ikeda M, Ide T, et al. Iron Overload via heme Degradation in the endoplasmic reticulum Triggers Ferroptosis in myocardial ischemia-reperfusion Injury. *JACC Basic Transl Sci*. 2022;7(8):800-819. [CrossRef]
7. Günes Günsel G, Conlon TM, Jeridi A, et al. The arginine methyltransferase PRMT7 promotes extravasation of monocytes resulting in tissue injury in COPD. *Nat Commun*. 2022;13(1):1303. [CrossRef].
8. Xie SS, Deng Y, Guo SL, et al. Endothelial cell ferroptosis mediates monocrotaline-induced pulmonary hypertension in rats by modulating NLRP3 inflammasome activation. *Sci Rep*. 2022;12(1):3056. [CrossRef]
9. Cristina Marcarini J, Ferreira Tsuboy MS, Cabral Luiz R, Regina Ribeiro L, Beatriz Hoffmann-Campo C, Ségio Mantovani M. Investigation of cytotoxic, apoptosis-inducing, genotoxic and protective effects of the fla onoid rutin in HTC hepatic cells. *Exp Toxicol Pathol*. 2011;63(5):459-465. [CrossRef]
10. Dong GZ, Lee JH, Ki SH, et al. AMPK activation by isorhamnetin protects hepatocytes against oxidative stress and mitochondrial dysfunction. *Eur J Pharmacol*. 2014;740:634-640. [CrossRef]
11. Chi G, Zhong W, Liu Y, et al. Isorhamnetin protects mice from lipopolysaccharide-induced acute lung injury via the inhibition

of inflamma ory responses. *Inflamm Res*. 2016;65(1):33-41. [CrossRef]
12. Sun M, Deng R, Wang Y, et al. Sphingosine kinase 1/sphingosine 1-phosphate/sphingosine 1-phosphate receptor 1 pathway: A novel target of geniposide to inhibit angiogenesis. *Life Sci*. 2020;256:117988. [CrossRef]
13. Gong G, Guan YY, Zhang ZL, et al. Isorhamnetin: a review of pharmacological effects. *Biomed Pharmacother*. 2020;128: 110301. [CrossRef]
14. Ren X, Han L, Li Y, et al. Isorhamnetin attenuates TNF-α-induced inflammation, proliferation, and migration in human bronchial epithelial cells via MAPK and NF-κB pathways. *Anat Rec (Hoboken)*. 2021;304(4):901-913. [CrossRef]
15. Li S, Cheng CS, Zhang C, et al. Edible and herbal plants for the prevention and management of COVID-19. *Front Pharmacol*. 2021;12:656103. [CrossRef]
16. Mura M, Cecchini MJ, Joseph M, Granton JT. Osteopontin lung gene expression is a marker of disease severity in pulmonary arterial hypertension. *Respirology*. 2019;24(11):1104-1110. [CrossRef]
17. Yu G, Wang LG, Han Y, He QY. clusterProfiler: an R package for comparing biological themes among gene clusters. *Omics*. 2012;16(5):284-287. [CrossRef]
18. Liu Z, Zhao Q, Zuo ZX, et al. Systematic analysis of the aberrances and functional implications of ferroptosis in cancer. *iScience*. 2020;23(7):101302. [CrossRef]
19. Zhou Y, Zhou B, Pache L, et al. Metascape provides a biologist-oriented resource for the analysis of systems-level datasets. *Nat Commun*. 2019;10(1):1523. [CrossRef]
20. Han H, Cho JW, Lee S, et al. TRRUST v2: an expanded reference database of human and mouse transcriptional regulatory interactions. *Nucleic Acids Res*. 2018;46(D1):D380-D386. [CrossRef]
21. Miao YR, Zhang Q, Lei Q, et al. ImmuCellAI: A unique method for comprehensive T-cell subsets abundance prediction and its application in cancer immunotherapy. *Adv Sci (Weinh)*. 2020;7(7):1902880. [CrossRef]
22. Miao YR, Xia M, Luo M, Luo T, Yang M, Guo AY. ImmuCellAI-mouse: a tool for comprehensive prediction of mouse immune cell abundance and immune microenvironment depiction. *Bioinformatics*. 2022;38(3):785-791. [CrossRef]
23. Zeng D, Li M, Zhou R, et al. Tumor microenvironment characterization in gastric cancer identifies prognostic and immunotherapeutically relevant gene signatures. *Cancer Immunol Res*. 2019;7(5):737-750. [CrossRef]
24. Wang J, Sun J, Liu LN, et al. Siglec-15 as an immune suppressor and potential target for normalization cancer immunotherapy. *Nat Med*. 2019;25(4):656-666. [CrossRef]
25. Deng S, Zhang Y, Wang H, et al. ITPRIPL1 binds CD3ε to impede T cell activation and enable tumor immune evasion. *Cell*. April 25 2024;187(9):2305-2323.e33. [CrossRef]
26. Davis AP, Wiegers TC, Johnson RJ, Sciaky D, Wiegers J, Mattingly CJ. Comparative Toxicogenomics Database (CTD): update 2023. *Nucleic Acids Res*. 2023;51(D1):D1257-D1262. [CrossRef]
27. Wiesmann C, Fuh G, Christinger HW, Eigenbrot C, Wells JA, de Vos AM. Crystal structure at 1.7 A resolution of VEGF in complex with domain 2 of the Flt-1 receptor. *Cell*. 1997;91(5):695-704. [CrossRef]
28. Sengoku T, Shiina M, Suzuki K, et al. Structural basis of transcription regulation by CNC family transcription factor, Nrf2. *Nucleic Acids Res*. 2022;50(21):12543-12557. [CrossRef]
29. Eberhardt J, Santos-Martins D, Tillack AF, Forli S, AutoDock V. AutoDock Vina 1.2.0: New docking methods, expanded force field, and python bindings. *J Chem Inf Model*. 2021;61(8):3891-3898. [CrossRef]
30. Warren C, Pavletich NP. Structure of the human ATM kinase and mechanism of Nbs1 binding. *eLife*. 2022;11. [CrossRef]
31. Ravindranath PA, Forli S, Goodsell DS, Olson AJ, Sanner MF. AutoDockFR: advances in protein-ligand docking with explicitly specified Binding Site fl xibility. *PLOS Comput Biol*. 2015;11(12):e1004586. [CrossRef]
32. Fu L, Shi S, Yi J, et al. ADMETlab 3.0: an updated comprehensive online ADMET prediction platform enhanced with broader coverage, improved performance, API functionality and decision support. *Nucleic Acids Res*. 2024;52(W1):W422-W431. [CrossRef]
33. Li B, Rui J, Ding X, Yang X. Exploring the multicomponent synergy mechanism of Banxia Xiexin Decoction on irritable bowel syndrome by a systems pharmacology strategy. *J Ethnopharmacol*. 2019;233:158-168. [CrossRef]
34. Ma C, Wang X, Zhang L, et al. Super enhancer-associated circular RNA-CircKrt4 regulates hypoxic pulmonary artery endothelial cell dysfunction in mice. *Arterioscler Thromb Vasc Biol*. 2023;43(7):1179-1198. [CrossRef]
35. Chakraborty A, Nathan A, Orcholski M, et al. Wnt7a deficit is associated with dysfunctional angiogenesis in pulmonary arterial hypertension. *Eur Respir J*. 2023;61(6) :1-47. [CrossRef]
36. Lan M, Wu S, Fernandes TM. Iron deficiency and pulmonary arterial hypertension. *Nutr Clin Pract*. 2022;37(5):1059-1073. [CrossRef]
37. Thenappan T, Ormiston ML, Ryan JJ, Archer SL. Pulmonary arterial hypertension: pathogenesis and clinical management. *BMJ*. 2018;360:j5492. [CrossRef]
38. Zhang DD. Mechanistic studies of the Nrf2-Keap1 signaling pathway. *Drug Metab Rev*. 2006;38(4):769-789. [CrossRef]
39. Mitsuishi Y, Taguchi K, Kawatani Y, et al. Nrf2 redirects glucose and glutamine into anabolic pathways in metabolic reprogramming. *Cancer Cell*. 2012;22(1):66-79. [CrossRef]
40. Pajares M, Jiménez-Moreno N, García-Yagüe ÁJ, et al. Transcription factor NFE2L2/NRF2 is a regulator of macroautophagy genes. *Autophagy*. 2016;12(10):1902-1916. [CrossRef]
41. Liu P, Dodson M, Li H, et al. Non-canonical NRF2 activation promotes a pro-diabetic shift in hepatic glucose metabolism. *Mol Metab*. 2021;51:101243. [CrossRef]
42. Anandhan A, Dodson M, Shakya A, et al. NRF2 controls iron homeostasis and ferroptosis through HERC2 and VAMP8. *Sci Adv*. 2023;9(5):eade9585. [CrossRef]
43. Yang JH, Shin BY, Han JY, et al. Isorhamnetin protects against oxidative stress by activating Nrf2 and inducing the expression of its target genes. *Toxicol Appl Pharmacol*. 2014;274(2):293-301. [CrossRef]